THE PENNSYLVANIA STATE UNIVERSITY
SCHREYER HONORS COLLEGE

DEPARTMENT OF BIOLOGY

INVESTIGATION OF DIRECT ASTROCYTE-TO-NEURON CONVERSION *IN VIVO* IN SPINAL CORD INJURY AND ALS MOUSE MODELS

AUSTIN REDILLA
SPRING 2018

A thesis
submitted in partial fulfillment
of the requirements
for a baccalaureate degree
in Biology
with honors in Biology

Reviewed and approved* by the following:

Gong Chen
Professor of Biology
Verne M. Willaman Chair in Life Sciences
Thesis Supervisor

Bernhard Lüscher
Professor of Biology
Professor of Biochemistry and Molecular Biology
Honors Adviser

* Signatures are on file in the Schreyer Honors College.

ABSTRACT

In cases of injury or disease, such as spinal cord injury (SCI) and Amyotrophic Lateral Sclerosis (ALS), the human central nervous system (CNS) has limited ability to repair itself through neurogenesis. One potential treatment would be to generate new neurons in these patients to replace the neurons dying from injury or disease. Previously, we have found the overexpression of NeuroD1 (ND1) in mature astrocytes is sufficient to reprogram these cells and transform them into adult, functional neurons. Herein, I have analyzed the utility of this astrocyte-to-neuron conversion technology in SCI and ALS mouse models. Both our stab injury and transgenic mouse models were able to accurately replicate the major pathological hallmarks of neuron loss, gliosis, and inflammation in reaction to injury and disease. In our SCI model, a suspension of viruses expressing the developmental genes NGN2, ISL1, and LHX3 was used to target astrocytes for conversion into motor neurons. In the area of viral infection a lower amount of neuron loss was observed 4 weeks post injury and some infected cells were identified as motor neurons. In our ALS model, the ND1 virus was expressed mostly in astrocytes at early time points, and mostly in neurons at later time points, suggesting conversion of astrocytes into neurons. Moreover, the discovery of cells in a transitional state from astrocyte to neuron and healthier appearing motor neurons in ND1 infected tissue further support the transformative and beneficial effects of the ND1 treatment. While these results are a promising start and begin to explain how ND1 and related transcription factors can be used in treating CNS injury and disease, more studies and a deeper investigation of the beneficial impacts are required to determine the full extent of its potential.

TABLE OF CONTENTS

LIST OF FIGURES

TABLE OF KEY ABREVIATIONS

AAV9	Adeno Associated Virus 9
ALS	Amyotrophic Lateral Sclerosis
ChAT	Choline Acetyltransferase
CNS	Central Nervous System
GFAP	Glial Fibrillary Acidic Protein
GFP	Green Fluorescent Protein
ND1	Neuronal Differentiation 1 gene
NIL	NGN2, ISL1, LHX3 solution of viruses
PBS	Phosphate Buffer Solution
PNS	Peripheral Nervous System
RFP	Red Fluorescent Protein
SCI	Spinal Cord Injury
SOD1	Super Oxide Dismutase 1

ACKNOWLEDGEMENTS

I would like to begin by thanking Dr. Chen for his generous supervision and mentorship over my last three and a half years in his lab. Through my time lab, I have turned from a young freshman with no research background into a veteran researcher with skill in a variety of basic and advanced research techniques. If it were not for Dr. Chen, I would never have had the opportunity to learn all of these skills and grow not only as a researcher, but as a person as well. Moreover, I would like to thank several of my other mentors that have had a significant impact on me along the way. I was introduced into the lab under Dr. Hedong Li and Brendan Puls, and I learned much of my skills from these mentors. Thank you, Dr. Li and Brendan, for your many years of support and guidance in the Spinal Cord Injury group.

I would like to particularly acknowledge the post-doctoral assistant who I have worked very closely with in the ALS group for the last year and a half, Yuan Liu. Yuan, you have sincerely helped me so much in all aspects of the research process. Your close guidance in organizing and designing my thesis was extremely appreciated. I thank you for your kind and patient teaching style and the warm friendship that we have developed.

Finally, I would like to acknowledge everyone else who, without their support, I would never have been able to complete this whole process. Of course, I would like to thank Dr. Chen and Dr. Lüscher for their time and their generous feedback for my thesis. I would like to thank Yuting Bai and Zifei Pei for their work in keeping the lab running smoothly and producing all of the virus used in our experiments. I would also like to thank Connor Kerstetter, Matt Keefe, Cody Forsyth, Matt Parry, Susan Huang, and Alice Cai for their friendship and their great help in collecting data. Last, but not least, I would like to thank my family and friends who have kept me

sane through all four years at Penn State. Mom, Dad, Devon, and Kate, thank you for always being there when I need to talk and encouraging me to keep pushing forward.

I am responsible for all of the work included in my thesis, except for the images which are labeled as being provided by Yuan Liu. For the images that were generously provided by Yuan, I was active in all other steps of the process for these samples, including surgery, injection, perfusion, sectioning, and imaging.

Chapter 1

Introduction

Spinal Cord Injury

Together, the brain and spinal cord comprise the central nervous system (CNS). Through infinitely complex connections and neural networks, these two systems provide the ability to think, reason, feel, and move, all of which are central to the human experience. Specifically, the spinal cord is largely responsible for the ability to feel and move, via the sensory neurons that are found in the dorsal horns of the spinal cord and the large motor neurons found in the ventral horns respectively. Injury to the spinal cord is a serious problem that impacts individuals across the world. It is estimated that there are roughly 23 cases of spinal cord injury (SCI) per million people worldwide, however the numbers range from 40 cases per million in North America to 15 cases per million in Australia [1].

SCI is a very serious condition, as any damage to the spinal cord can cause severe deficits in sensation and movement. In North America, 60% of SCI cases are a result of either a motor vehicle accident or a fall, however violence, sports, and medical/surgical accidents also have a meaningful share [2]. Since 2015, 67% of those with SCI suffered from incomplete paralysis where some form of sensation or movement did remain, while 32% suffered from complete para- or tetraplegia resulting from a complete spinal cord lesion [2].

The mechanism of injury and cell damage from SCI takes place in two stages: a primary stage consisting of the initial deformation of tissue caused by the trauma and a secondary stage

consisting of various biochemical reactions to the injury [3]. Important secondary mechanisms include cell death, vascular changes, inflammation, and edema. In addition, reactive gliosis in the area of the injury often leads to the formation of a glial scar. While the scar is able to control the local immune response and provide a protective barrier from the toxicity of the injured area, the dense population of reactive glial cells prevents the growth of axons, essentially retarding the ability for natural repair [4,5].

Amyotrophic Lateral Sclerosis

Amyotrophic Lateral Sclerosis (ALS) is a chronic neurodegenerative disease which results in the gradual death of lower motor neurons in the spinal cord and upper motor neurons in the brain. This initially manifests as weakness and difficulty with movement and ultimately results in death, typically from respiratory failure 20–48 months after disease onset [6]. In European populations, where the disease is most prevalent, the incidence is estimated to be 3 new cases per 100,000 people per year, with an overall lifetime risk of 1:350 for men and 1:400 for women [7]. ALS can be passed down through families in a genetic manner, or it can develop sporadically through environmental interactions. It is estimated that 17–23% of cases follow a familial pattern of inheritance. Among familial ALS, mutations in the super oxide dismutase gene SOD1 are the most correlated with the disease, however variants in the genes FUS and TARDBP are also common contributors [8]. Despite representing the majority of cases, the exact causes of sporadic ALS remain elusive. The complex relationships between genes and environment and the infinite number of environmental variables have made it difficult to pin down specific causes of sporadic ALS [7].

Despite differing modes of onset, many of the pathological characteristics of ALS are shared among familial and sporadic cases. An early model for ALS pathogenesis identified glutamate excitotoxicity as a main contributor to motor neuron death [9]. Essentially, mutant glial cells are unable to remove the excitatory neurotransmitter glutamate fast enough from the post-synaptic space of motor neurons, causing an excess of action potential firing and an influx of Ca^{2+} into the neurons, which is toxic. Further studies have identified several other important pathological markers in ALS, including activation of microglia, axonal disorganization, and a prion-like spread of misfolded proteins in a cell-to-cell manner [9].

Current treatments for ALS are few and far between. In 1995, the first drug to be approved for clinical treatment was riluzole, a presynaptic glutamate inhibitor. Attempting to control the disease by lessening the load of glutamate excitotoxicity, riluzole proved to be mildly effective, prolonging lifespan on average by two to three months [10]. It took more than twenty years for the next drug to be approved for treatment, edaravone [11]. By attacking reactive oxygen species and lessening the oxidative stress on neurons of ALS patients, edaravone has been shown to slow the progression of the disease [12]. The relatively small number of approved drugs and their mild efficacy suggests there is a strong need for more numerous and effective treatments to fight ALS.

Direct Astrocyte-to-Neuron Conversion

A new era of medical research was ushered in when the first induced pluripotent stem cells (iPSCs) were generated from mouse, and later human, fibroblasts [13,14]. By introducing a simple set of four transcription factors into the nucleus of these cells, differentiated fibroblasts

were reverted to pluripotent stem cells, allowing them to re-develop into nearly any cell type. This discovery became especially important in neuroscience research because of the limited ability for the human body to regenerate neurons after disease or injury. Indeed, several types of neurons derived from iPSCs, including dopamine and gamma-Aminobutyric acid (GABA) producing neurons, have been transplanted into different animal models, such as Parkinson's disease and stroke, as potential treatments [15,16]. Despite the technique's great promise, it has some limitations as well. Firstly, there is the potential for immune rejection of the transplanted pluripotent cells by the host, which has dampened the success of using iPSC derived neurons as treatments for neurological diseases [17]. iPSC transplantation has other drawbacks including the extensive time and work needed to differentiate a large number of cells in culture as well as potential tumorigenesis of undifferentiated cells after transplantation [18,19].

One method to overcome the these limitations is to bypass the pluripotent stem cell phase and directly convert one adult cell type to another *in vivo*. Cellular reprograming can be achieved by altering the transcriptional profile of a differentiated cell to match that of a different cell type. Typically, a viral vector is used to deliver a desired gene from one cell type directly to a mature cell of a different type. In pioneering research conducted in our lab, it was shown that delivery of a single transcription factor, NeuroD1 (ND1), was able to directly convert astrocytes into functional neurons *in vivo* [20]. Since then, the field of cellular reprogramming has expanded to find several transcription factors, microRNAs, and even small molecules that are able to directly reprogram one cell type into another [21,22].

Two of the most promising candidates for neuronal cell reprograming are the key developmental transcription factors ND1 and Neurgenin2 (NGN2) [23,24]. ND1 is a member of the basic helix-loop-helix transcription factor family, which are responsible for determining the fate

of cells. Expressed late in the development of neurons, ND1 is associated with neuronal differentiation, maturation, survival, and even adult neurogenesis [25–27]. NGN2 is also part of the basic helix-loop-helix family, and is a key player in the differentiation of spinal cord neurons. NGN2's expression is involved in the pathway for the formation of spinal dorsal horn interneurons, however it is most directly involved in spinal motor neuron differentiation [28,29]. Both of these master transcription factors begin a cascade of downstream transcriptional factors typically found in developing neurons to drive reprogramming from one cell type, like astrocytes, into neurons.

As a therapy, direct cellular reprogramming holds a tremendous amount of promise to treat neurodegenerative diseases. Where the human nervous system fails to provide a readily available, renewable supply of neurons in the case of disease or damage, cellular reprograming can step in and provide a new source of neurons generated directly from the patient's own cells *in vivo.* Current work in our lab and around the world is being done to apply this therapy in various disease and injury models including stroke, Alzheimer's, Huntington's, SCI, and ALS.

Chapter 2

Materials and Methods

Viral Vector

To deliver transcription factors such as ND1, NGN2, and others, a system using adeno associated virus 9 (AAV9) was used (Figure 1). Briefly, the cre recombinase enzyme was packaged into the AVV9 virus behind the human Glial Fibrillary Acidic Protein (hGFAP) promoter. As GFAP is typically expressed in astrocytes, the cre recombinase should only be expressed in astrocytes infected by the virus. Additional viruses were also generated with other genes of interest, including ND1-mCherry and NGN2-mCherry for experimental groups and mCherry-mCherry for control groups. Instead of the hGFAP promoter, these genes were packaged behind the CAG promoter, which is constitutively active in all cell types. In addition, these sequences were inverted and located between two flip-excision (FLEx) loxP sites, which are the natural splice targets for the cre recombinase enzyme. Inversion to the proper orientation, and therefore expression, of the desired sequences can only occur in the presence of cre recombinase. The viruses were introduced to human embryonic kidney (HEK) 293T cells where they proliferated and were then isolated by centrifuge for 2hrs at 4 °C. Viruses were produced by Zifei Pei for the lab.

For experimentation, the AAV9-GFAP::cre and AAV9-CAG::FLEx viruses were mixed together into a single solution. In theory, this would ensure that only astrocytes expressing GFAP would produce cre and therefore be able to invert the desired genes on the CAG::FLEx virus to their proper orientation, allowing for gene expression.

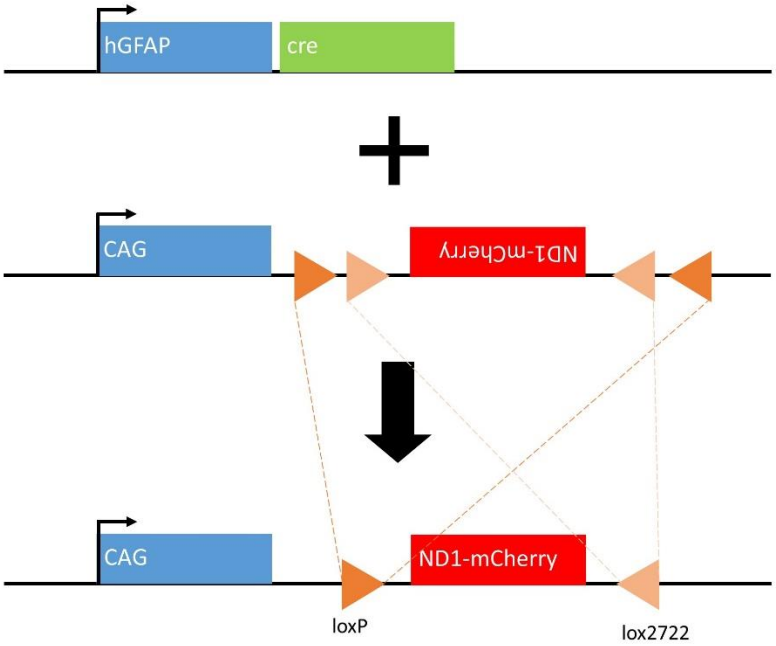

Figure 1. Graphical Depiction of AAV9 Virus Scheme

Only when both viruses carrying cre recombinase and ND1-mCherry infect the same cell can the ND1-mCherry sequence be inverted to its proper orientation and expressed

Laminectomy

To gain access to the spinal cord for induction of the stab injury or stereotaxic injection, a laminectomy, or removal of the back of the vertebrae, was performed. Mice were initially weighed and put under anesthesia via an intraperitoneal (IP) injection of a ketamine and xylazine solution. The final dosage to the mouse was given at 120 mg/kg ketamine and 16 mg/kg xylazine. After loss of consciousness, the mice were prepared by shaving a clean area on their back and disinfecting the area with betadine and 70% ethanol. Artificial tears were administered to prevent the eyes of the mice from drying out while unconscious, and local analgesic was given in the form of a 10 mL/kg subcutaneous injection of 4 mg/kg of bupivacaine in the prepared area

of the back. A scalpel was then used to make a midline incision down the spine. Small cuts between the spaces of the T11-L1 vertebrae were made using the scalpel to separate the lamina from connecting muscle and tissue. Finally, a curved pair of scissors was placed between the vertebrae and spinal cord and used to remove the lamina of the T11-L1 vertebrae, revealing a rectangular bone window with direct access to the spinal cord.

After the stab and/or stereotaxic injection was performed, the incision wound was closed using polyglycocidic acid absorbable sutures. A subcutaneous injection of 5 mg/kg of carprofen was given as an analgesic and IP injections of 1mL Saline solution and 0.1 mL atipamezole were given for hydration and sedative reversal, respectively. Finally, the mice were left to recover in a clean cage heated by an electric heating pad and were monitored until consciousness was regained.

SCI Model and Stereotaxic Injection

A 26 gauge needle was used after the laminectomy procedure to induce a stab injury in the mice. Fastened to the stereotaxic injecting machine, the 26 gauge needle was initially lined up at the midline of the spinal cord inside of the bone window. From the midline, the needle was positioned 0.45 mm laterally to the left or right to target the lateral motor column in the ventral horn of the spinal cord. Another needle was used to cut a small slit in the dura of the spinal cord and then the 26 gauge needle was inserted to a depth of 1.3 mm and held for 30sec to induce the stab injury. After holding for the required amount of time, the needle was withdrawn slowly so not to induce any further injury beyond the stab itself. Between stabs, the needles were rinsed

with deionized water to ensure they were not blocked with blood or tissue and sanitized with an alcohol wipe.

If a mouse was intended to undergo a stereotaxic injection of virus after the stab, a 5 µL Hamilton Syringe was loaded with 1 µL of pre-prepared virus and fastened to the stereotaxic injecting machine. Using the stab site as a reference point, the 34 gauge injection needle was lined up anywhere from 1-2 mm away from the injury core, depending on the goals of the specific experiment. Again, the needle was placed 0.45mm laterally from the midline on the same side as the stab injury. After making a small slit in the dura, the injection needle was lowered to a depth of 1mm and the virus was delivered at a rate of 0.1 µL per minute. Following the ten minutes of injection, the needle was left to rest in place for two minutes to allow the virus time to spread and then withdrawn slowly. For ALS mice, the procedure remained the same except the injection needle was initially lined up at the midline in the middle of the bone window rather than at the site of a stab injury. Post-operative care followed the procedure as given in the Laminectomy section.

ALS Model

A transgenic mouse line (JAX stock#002726) hemizygous for the G93A mutation of the human SOD1 gene was purchased from Jackson Labs to serve as a mouse model for ALS [30,31]. Hemizygous males were mated with wildtype C57BL/6J females to produce hSOD1-G93A^{+} offspring. All litters were weaned from their parents by three weeks of age, when a skin sample was taken to run PCR tests to confirm the presence of the mutation. Those mice who clearly

showed to be carrying the mutated gene were used for experiments, while those who were negative or inconclusive were discarded from experimentation.

As the mice aged, various behavior tests and scales were used to monitor the progress of the disease. The RotaRod was used to determine ambulatory ability by challenging the mice to walk on a rotating bar. The bar was kept at a constant speed of 14 rpm and a maximum experiment time was set at 180 seconds. The mice walked for as long as they could until they fell off and completed three trials each week. To reduce error, mice were trained three times on the RotaRod by completing a full three minute run before data was officially collected, usually around 12 weeks old. To test their grip strength, a hangwire test device was developed by a previous lab member, Matthew Keefe. The mice were placed on a thin metal cage and flipped upside down, forcing them to hold their own bodyweight to stay suspended. The mice completed two trials every week where the amount of time they could hold onto the cage was recorded, up to a maximum of 120 seconds. Finally, a third measure used a five-point behavior scale to assess the mice towards the end of their life. A humane endpoint was determined to be when the mice could no longer right themselves from lying in a position on their sides. At this stage, the mice were euthanized and prepared for tissue collection.

Tissue Preparation and Sectioning

Transcardial perfusion was used to fix the spinal tissue of the mice. Mice were anesthetized with 0.3 mL of avertin (1 g 2-2-2-tribomoethanol; 1 mL 2-methyl-2-butanol; 39 mL 1xPBS) administered via IP injection. They were then fixed into a cork board and opened up at the area of the sternum. The diaphragm was cut and the ribcage pulled back to visualize the

heart. Using a 28 gauge needle, the left ventricle of the heart was pierced and normal saline solution was pumped into the heart. Simultaneously, the right atrium was ripped open with a pair of forceps, draining the blood from the animal while it is being replaced with the normal saline solution. The color of the liver was used as an indicator to determine when all of the blood was replaced with saline solution. After the liver turned completely pale due to lack of blood, the pump was stopped and the input tube was transferred from normal saline solution to 4% paraformaldehyde. 40 mL of 4% paraformaldehyde was then pumped into the heart to initially fix the tissue.

After perfusion, the mice were transferred to a separate stage for dissection of the spinal cord. Once removed, the spinal cord sample was left in 4% paraformaldehyde overnight for further fixation, and then submerged in 30% sucrose for 72 hrs for dehydration.

Following the tissue preparation, spinal cord samples were sectioned using a Leica Cryostat. Frozen within a solid block of cryomatrix, thin samples of 20–40 μm in thickness were cut in horizontal and coronal fashions. Each section was carefully maneuvered within the machine and pressed on to a positively charged glass slide where it became adhered in place. On a single slide, anywhere from 6–20 spinal cord sections were collected, depending upon the requirements of the specific experiment. The glass slides were stored inside of a slide box in a -30 °C freezer for short term use (within 3 months) and -80 °C for longer term storage (>3 months).

Immunostaining and Imaging

Immunostaining was used to visualize various cell markers within the prepared tissue sections. Briefly, the slides were immersed in 1x phosphate buffer solution (PBS) 3 times for 5 minutes each to wash the spinal cord samples of excess cryomatrix from tissue sectioning. Afterwards, a hydrophobic wax border was drawn around the tissue samples directly on the slide using a wax depositing pen. Within the hydrophobic box, 150 µL of blocking solution (2.5% normal donkey serum (NDS)/2.5% normal goat serum (NGS)) was added to block non-specific binding sites and the samples were left to incubate for 1 hour. Primary antibody solutions were prepared by diluting the antibodies to their required ratios in the same 2.5% NDS/NGS solution as the blocking solution. After one hour of blocking, the blocking solution was removed, and the primary antibody solution was added to incubate for two nights at 4 °C.

After two nights, the primary solution was removed and the slides were washed 3 times with 1xPBS before a secondary antibody solution was added. The secondary solution consisted of antibodies conjugated with fluorophores (Alexa 647, 546, 488) diluted to a concentration of 1:800 in the original blocking solution. After incubating for 2 hrs at room temperature in the secondary solution, the slides were washed 3 times again in 1xPBS and mounted with a coverslip using Gold Anti-fade Mounting Solution.

All images were collected using Zeiss and Olympus Confocal microscopes.

Chapter 3

Results

Characterization of Stab Model

A standardized stab model was established using a 26 gauge needle to induce a stab injury in the lumbar spinal cord of wildtype mice. Significant neuron loss and astrogliosis was observed early on, just 4.6 days post-stab (dps), and later on at 4 weeks post-stab (wps) (Figure 2A). At 4.6 dps, a large number of neurons were found to be missing in the area of the stab, however neuron loss was not seen in the contralateral side of the spinal cord. In addition, there was a large amount of reactive astrocytes observed. A dense area of gliosis was found in the area of neuron loss, however reactive astrocytes were found throughout the length of the spinal cord sample, suggesting the injured environment is larger than the specific area of neuron loss. By 4 wps, the area of neuron loss had grown and some neuron loss was observed in the opposite side of the spinal cord as the stab (Figure 2A). Astrogliosis had advanced to a more severe stage than the 4.6 dps sample and a glial scar formed in the area of the greatest neuron loss. Finally, some tissue necrosis was also observed in the 4 wps sample, consistent with typical SCI pathology over an extended period of time. High magnification images further confirmed the presence of hypertrophic astrocytes and the relative absence of surviving neurons in the damaged area at both time points (Figure 2B).

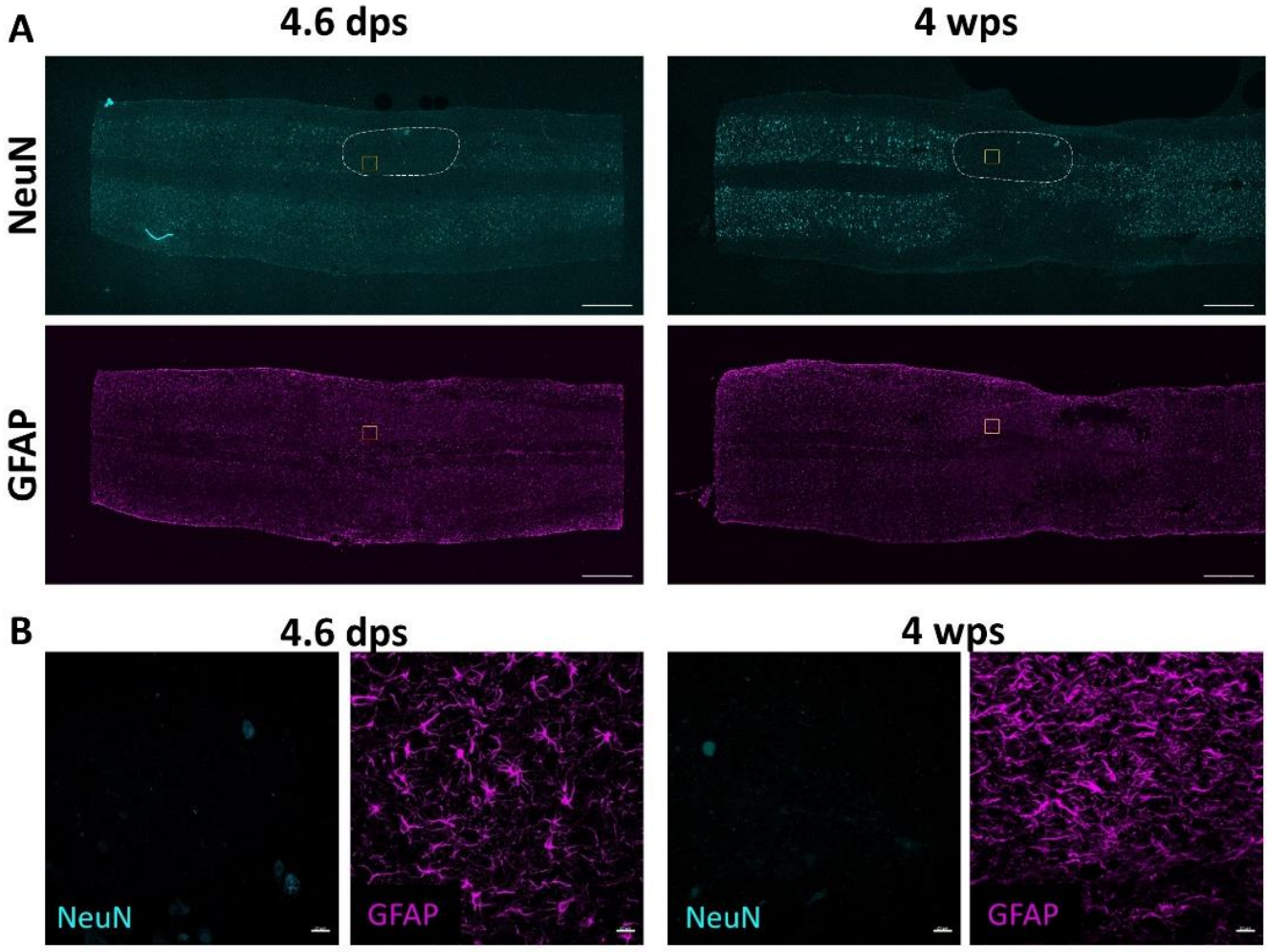

Figure 2. Basic Pathological Markers of SCI
(A**)** Overview of neuron loss and astrogliosis at early (4.6 days) and late (4 weeks) time points post stab injury. White boxes outline areas of severe damage. These areas have significant neuron loss, visualized by the lack of the neuronal nucleus marker, NeuN, and severe gliosis, visualized by hypertrophic astrocytes using the glial marker GFAP. Scale bar is 500 μm **(B)** High magnification images taken from inside the area of severe damage highlighting the loss of neurons and morphology of reactive astrocytes. Scale bar is 20 μm. Images provided by Yuan Liu

NIL Virus Injection in SCI

In order to investigate astrocyte-to-neuron conversion in the SCI model, a solution of viruses designed to express the three transcription factors NGN2, ISL1, and LHX3 (NIL) was

used because it is known that these transcription factors play an important role in motor neuron development [32]. The viruses carrying the transcription factors were designed with an mCherry tag to visualize the infection of cells in the spinal cord.

At 4.6 dps, a large amount of neuron loss was observed in the NIL sample when compared to the control sample at the same time point (Figure 3A). A number of variables, such as the development of a hematoma or infection could have resulted in such different injuries. Despite this variation, significant differences can be seen in the expression of mCherry in the NIL sample when compared to the control sample. All of the infection in the control sample was observed in astrocytes, while some could also be observed in neurons in the NIL injected sample (Figure 3B). In fact, a large majority of the surviving neurons in the damaged area of the NIL sample at 4.6 dps were infected with the NIL virus. At 4 wps, the difference was more dramatic. Many neurons were observed within the severely damaged area of the NIL sample at 4 wps, while little to no neurons were found in the damaged area of control sample at this time point (Figure 3A). In the control sample, high magnification images were able to show the majority of the infection was found in astrocytes; but, in the 4wps NIL injected sample, the majority of the infection was found in neurons (Figure 3B).

It is important to make a distinction between the damaged area, indicated by severe neuron loss and astrogliosis, and its surrounding area. Especially at 4 wps, the virus appeared to act differently in both of these regions (Figure 3A). In the mCherry control sample, the virus appears to have the ability to infect neurons in the surrounding area, but not in the damaged area. The control virus should not have the ability to infect neurons; thus, these mCherry+ neurons in the control sample are leaked cells that are incorrectly infected by the virus. Because there

appears to be a large amount of leakage in the surrounding area of the stab but not in the heavily damaged area, further analysis of the NIL infection was exclusively limited to the damaged area.

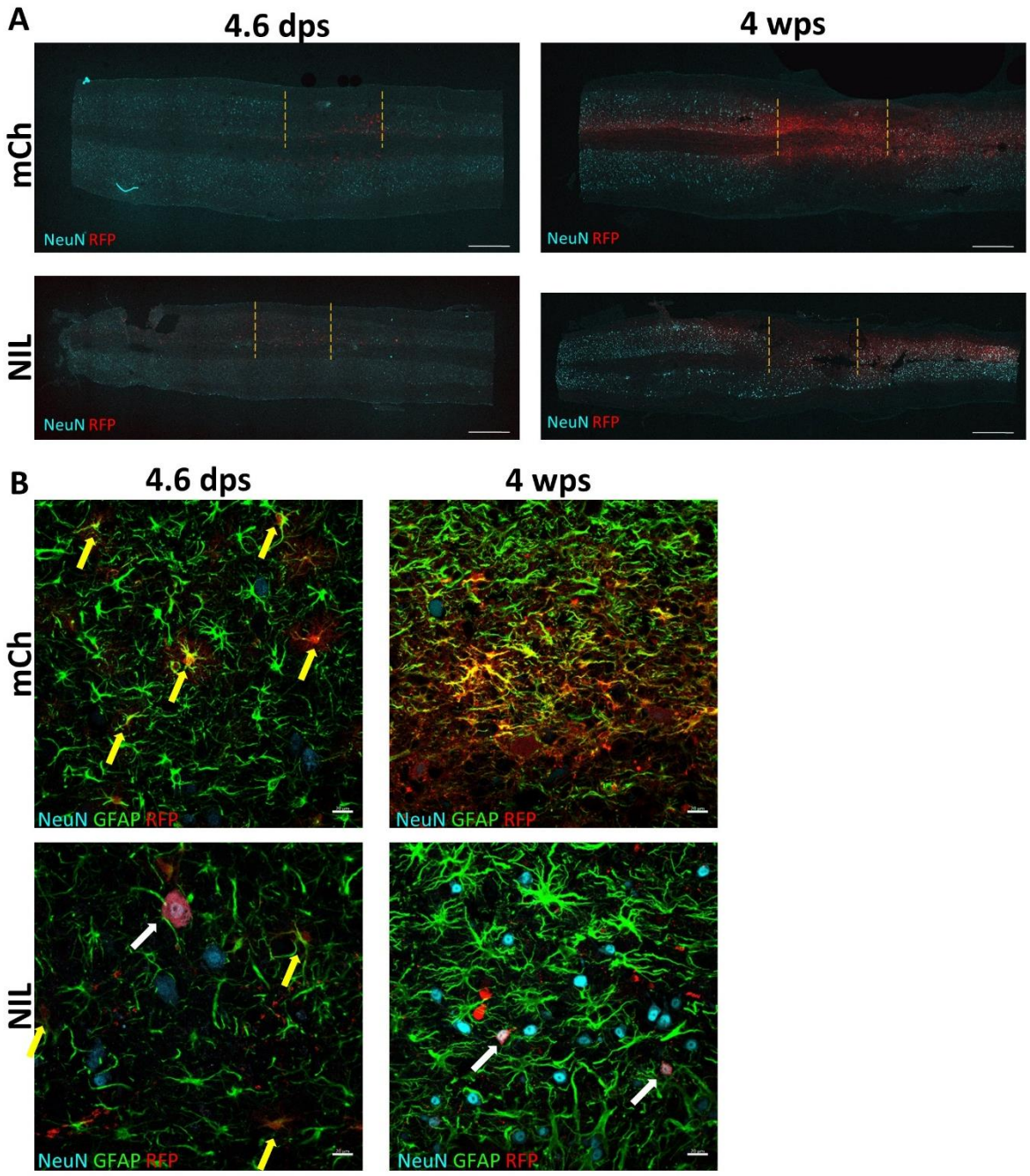

Figure 3. NIL Infection can be Observed in Neurons Inside of the Damaged Region
(A) Overview of neuron loss and infection status in mCherry control group and NIL experimental group at early (4.6 days) and late (4 weeks) stage post stab injury and virus injection. Yellow lines indicate areas of severe damage, as

confirmed by significant neuron loss and gliosis. Scale bar is 500 μm **(B)** High magnification images showing population of infected cells by each virus. Yellow arrows mark infected astrocytes that express both the glial marker GFAP (green) and the AAV9 reporter protein mCherry (red). White arrows indicate cells which co-express the neuronal marker NeuN (blue) and mCherry (red). Yellow arrows were excluded from the mCherry 4 wps image because almost all of GFAP expressing astrocytes expressed the mCherry reporter protein as well. Scale bar is 20 μm. Images provided by Yuan Liu.

A closer examination of the 4.6 wps NIL-mCherry injected mouse reveals possible newly generated motor neurons. Within the severely damaged area of the spine where a glial scar has formed, several neurons can still be observed at 4 wps (Figure 4A). Within this damaged area, infection of cells by the NIL virus was seen (Figure 4B). Specifically, a cell with neuronal morphology in this area was found to co-stain with NeuN, mCherry, and Choline Acetyltransferase (ChAT) (Figure 4C). The presence of several cholinergic synapses across its body is similar to that of a wildtype spinal motor neuron, indicating that the infected cell is a motor neuron. There are two possible explanations for this observation: either the infected motor neuron is a newly generated motor neuron or it is an endogenous motor neuron infected by the NIL virus through leakage. Both possibilities will be discussed further in the discussion section.

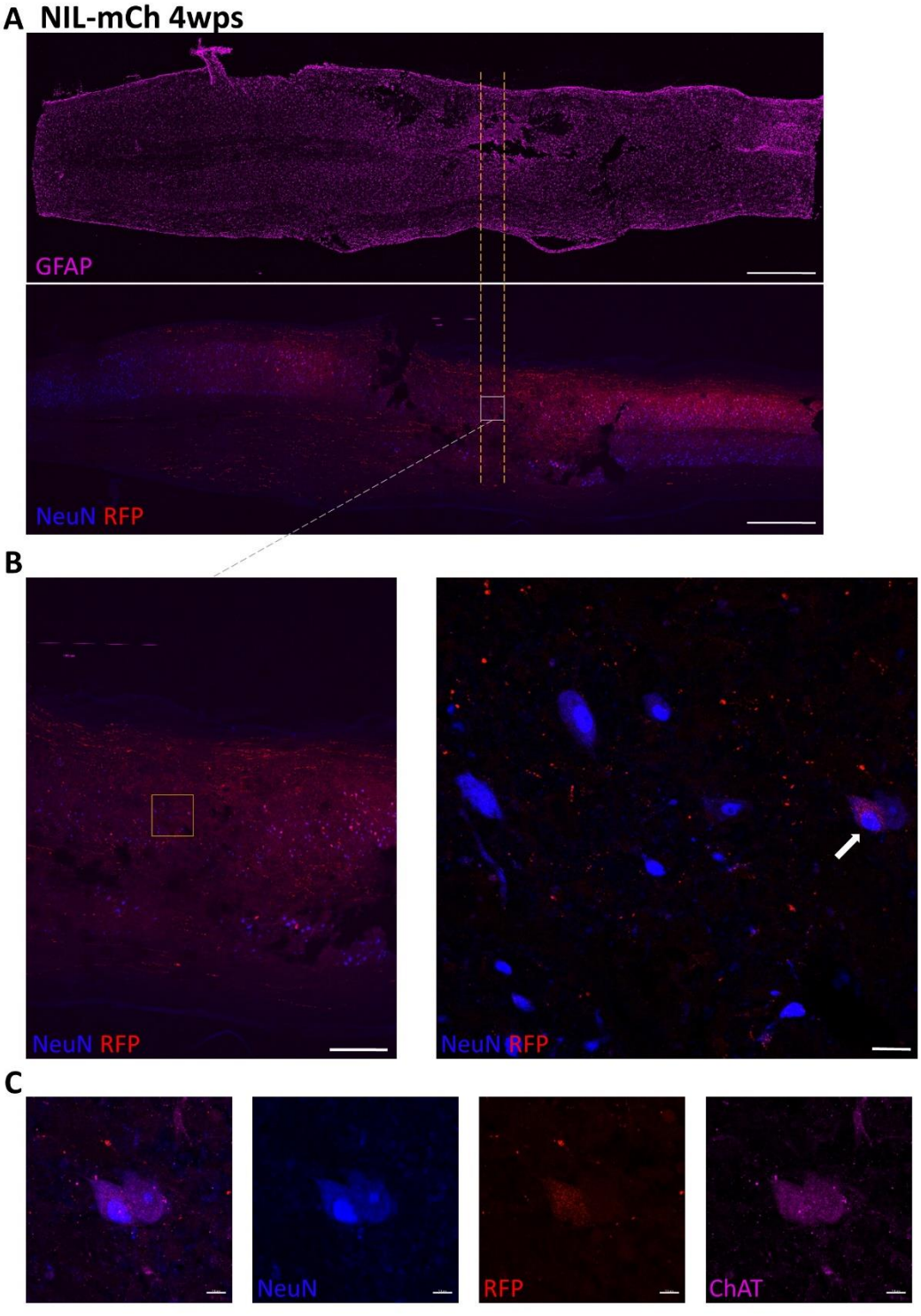
A NIL-mCh 4wps
GFAP
NeuN RFP
B
NeuN RFP
NeuN RFP
C
NeuN
RFP
ChAT

Figure 4. Motor Neuron Characterization in NIL Injected SCI Model
(A) Overview of NIL-mCherry infection and gliosis status 4 weeks after stab injury. The dashed yellow lines are shown to highlight that the high magnification images are taken within the area of extreme gliosis and neuron loss. Scale bar is 500 μm **(B)** 20x imaging showing a neuron expressing the neuronal marker NeuN (blue) and the AAV9 mCherry reporter protein (red). Scale bars are 200 μm (right) and 50 μm (left). **(C)** Characterization of mCherry expressing neuron as a motor neuron using the cholinergic terminal marker ChAT (purple). Scale bar is 20 μm. Images provided by Yuan Liu

Characterization of ALS Mouse Model

Three main pathological markers of ALS include selective motor neuron death, increased immune activity via microglia ,and activation of reactive astrocytes [31,33,34]. In our SOD1 G93A mouse model of ALS, we were able to observe all of these cellular changes as the disease progressed (Figure 5A). As the age of the mice increased, fewer numbers of motor neurons were visible via NeuN in the lateral motor column of the ventral horn of the spinal cord, indicating motor neuron death. CNS immunoreactivity was shown to increase as well, with Iba1 staining revealing a progressive increase in microglia as the mice aged. GFAP staining revealed reactive astrocytes were present as early as 8.9 weeks in these mice, and persisted at high levels throughout the course of their life.

Moreover, our model mimicked the pathogenesis of the misfolded SOD1 protein model of ALS very well. In the natural disease, cytoplasmic concentrations of the misfolded protein will increase within motor neurons until intracellular occlusions begin to form, which will ultimately results in apoptosis and cell death [35]. In our model, significant concentrations of the misfolded protein can be seen at 12.7 wks, while inclusions within motor neurons were observed as early as 15.1 wks (Figure 5B).

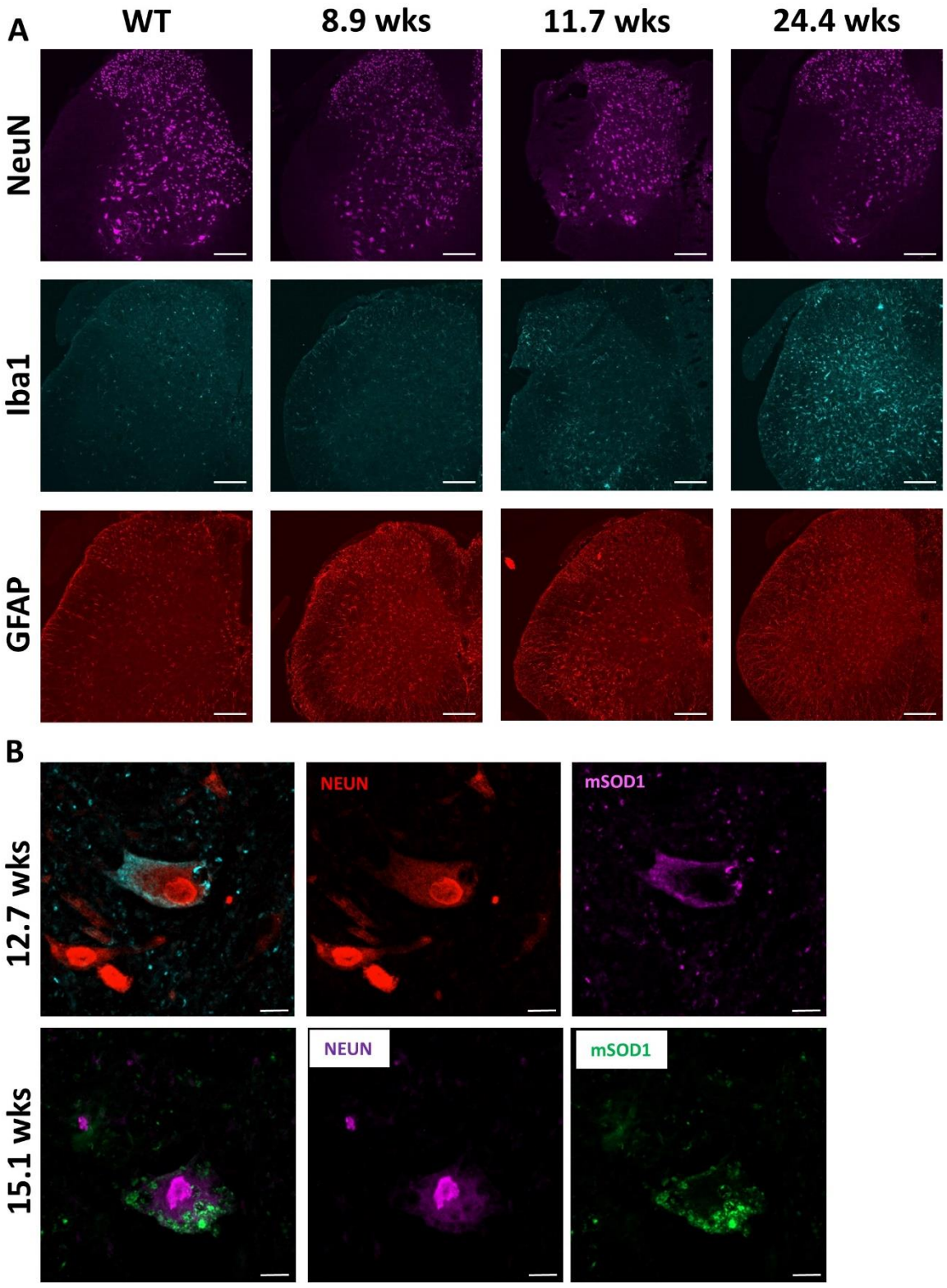
A
WT
8.9 wks
11.7 wks
24.4 wks
NeuN
Iba1
GFAP
B
12.7 wks
NEUN
mSOD1
15.1 wks
NEUN
mSOD1

Figure 5. Basic Characterization of ALS Mouse Model
(A) Loss of motor neurons in the ventral horn visualized by neuronal marker NeuN (purple), increased immune activity visualized by microglia marker Iba1 (blue), and reactive gliosis visualized by astrocyte marker GFAP (red) in one side of spinal cord shown in a wildtype mouse and at various stages during disease progression. Scale bars are 200 μm **(B)** cytoplasmic misfolded SOD1 protein is visible diffusely in the cytoplasm of motor neurons at 12.7 wks and as intracellular inclusions at 15.1 wks. Scale bars are 20 μm. Images for (B) were provided by Yuan Liu

In addition to the basic markers of ALS and other neurodegenerative diseases, our ALS mouse model was able to replicate more specific pathological changes. The identification of these changes is important as they further support the SOD1 G93A mice as an accurate ALS model and provide different targets to determine the success of treatments. One such change is the significant reduction in the vesicular glutamate transporter, vGlut1, perhaps due to the excitotoxic death of neurons receiving glutamatergic inputs [36]. In our model, a reduction was also seen in vGlut1 with progression of the disease, particularly in the ventral horn and medial spinal cord (Figure 6A). Further investigation with high magnification imaging showed that surviving motor neurons in SOD1 mice do retain glutamatergic synapses at 24 weeks of age, however their density is reduced when compared to wildtype motor neurons (Figure 6B). Moreover, the glutamatergic synapses at 24.4 weeks of SOD1 mice displayed a reduced intensity of vGlut1 staining when compared to the wildtype, suggesting a lower concentration of vGlut1 in surviving glutamatergic synapses at this time point.

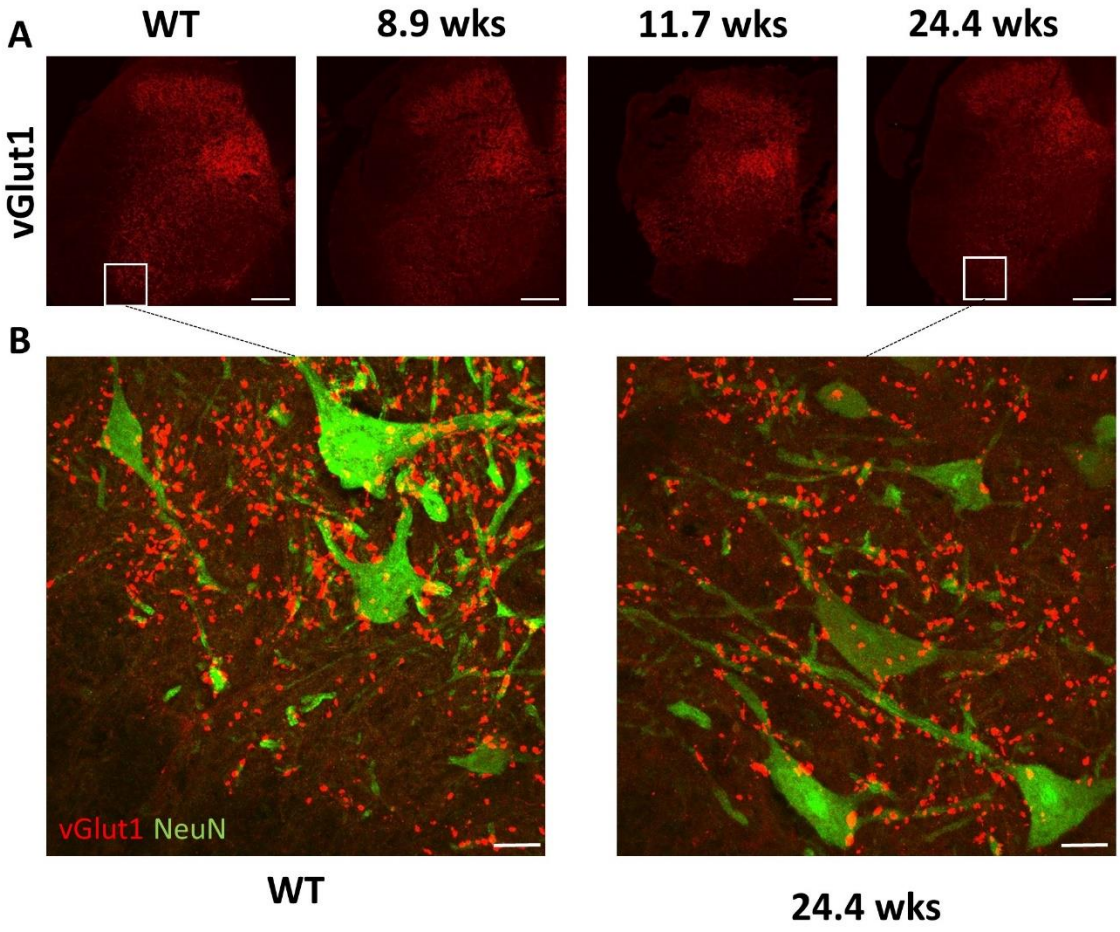

Figure 6. Reduction of vGlut1 in ALS Mouse Spinal Cord with Disease Progression
(A) Immunohistohemical imaging of the glutamatergic synapse marker vGlut1 (red) in the spinal cord. Reduced vGlut1 was seen in the ventral horn and medial sections of the spinal cord in aging SOD1 G93A mice. Scale bars are 200 μm **(B)** 60x imaging of the ventral horn shows reduced density and intensity of vGlut1 surrounding motor neurons (green) in SOD1 G93A mice. Scale bars are 20 μm

Another important marker of ALS is the degernation of the peripheral nervous system (PNS) secondary to the CNS. As the direct link between the CNS and motor output, the PNS is important to study because there will be no behavioral improvement in ALS without improvement to the PNS as well. With ALS, misfolded SOD1 proteins have been shown to collect in the axons of neurons running through the sciatic nerve, the main nerve providing input to the muscles of the legs. This causes severe disruptions to the axons and the mylein sheath

surrounding them [37]. In our model, myelin degernation in the sciatic nerve was seen as early as 8.9 weeks with lipid ovoid formation, and by 21.3 weeks complete demylenation of many axons was observed (Figure 7A). In addition, large misfolded SOD1 inclusions were found in areas of severe axonal degeneration, while healthier axons were spared (Figure 7B).

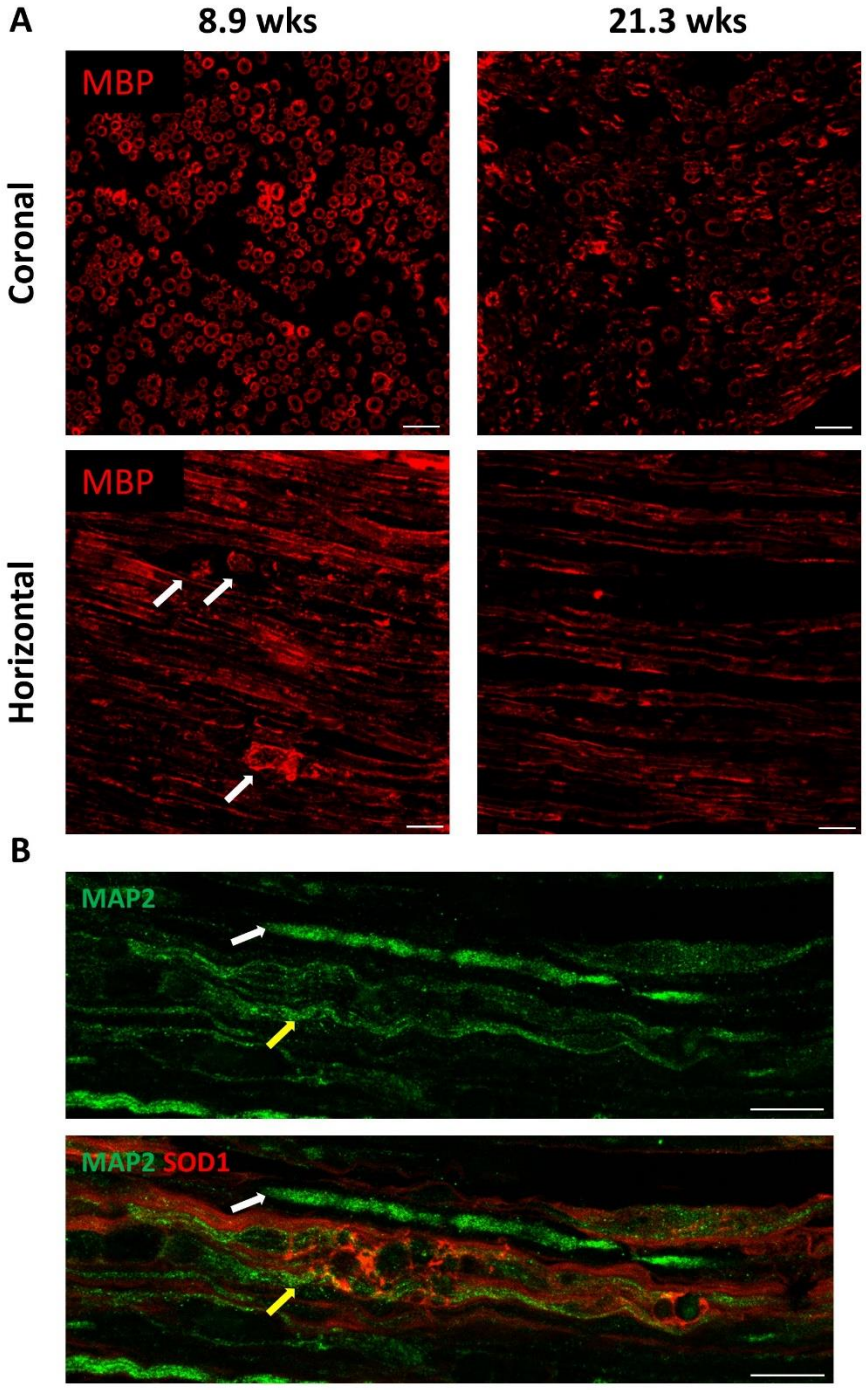

Figure 7. Peripheral Nerve Degeneration in ALS Mouse Model
(A) Myelin basic protein (MBP) staining of the SOD1 G93A mouse sciatic nerve at 8.9 and 21.3 weeks. At 8.9 wks, lipid ovoids are observed (white arrows), and at 21.3 wks complete demyelination can be seen as whole segments of MBP are missing. Scale bars are 20 μm **(B)** 60x imaging of 21.3 wk SOD1 G93A horizontal sciatic nerve sections.

Healthy axons (white arrow) show little to no misfolded SOD1, while degenerated axons (yellow arrow) present with large SOD1 inclusions. Scale bars are 20 μm

ND1 Injection in ALS Mouse Model

In an initial experiment to test the effect of ND1 in the ALS mouse model, a two sided virus injection was planned. On one side of the spinal cord, a solution containing AAV9 GFAP::cre and AAV9 CAG::FLEx-ND1-mCherry (AAV9 GC//F-ND1-mCh) was injected into the ventral horn. On the other side a solution containing AAV9 GFAP::cre and AAV9 CAG::FLEx-GFP (AAV9 GC//F-GFP) was injected. In this way, one side was able to operate as the experimental condition and the other the control condition. SOD1 G93A mice were injected around 8 weeks of ages, when some molecular signals are beginning to present, and sacrificed two weeks later to observe the infection status. At this time point, it was observed our stereotaxic injection techniques were successful in targeting the ventral horns in a two sided injection (Figure 8A). Very different expression patterns were seen between the GFP control and ND1 injection. Much of the GFP infected cells presented in astrocytic morphology and did not co-satin with NeuN, while the ND1-mCherry infected cells presented with neuronal morphology and largely co-stained with NeuN (Figure 8B). The results of this experiment suggest our AAV9 GFAP::cre system successfully targets astrocytes, and our ND1 virus is able to convert the initially infected astrocytes into neurons by 2 wpi.

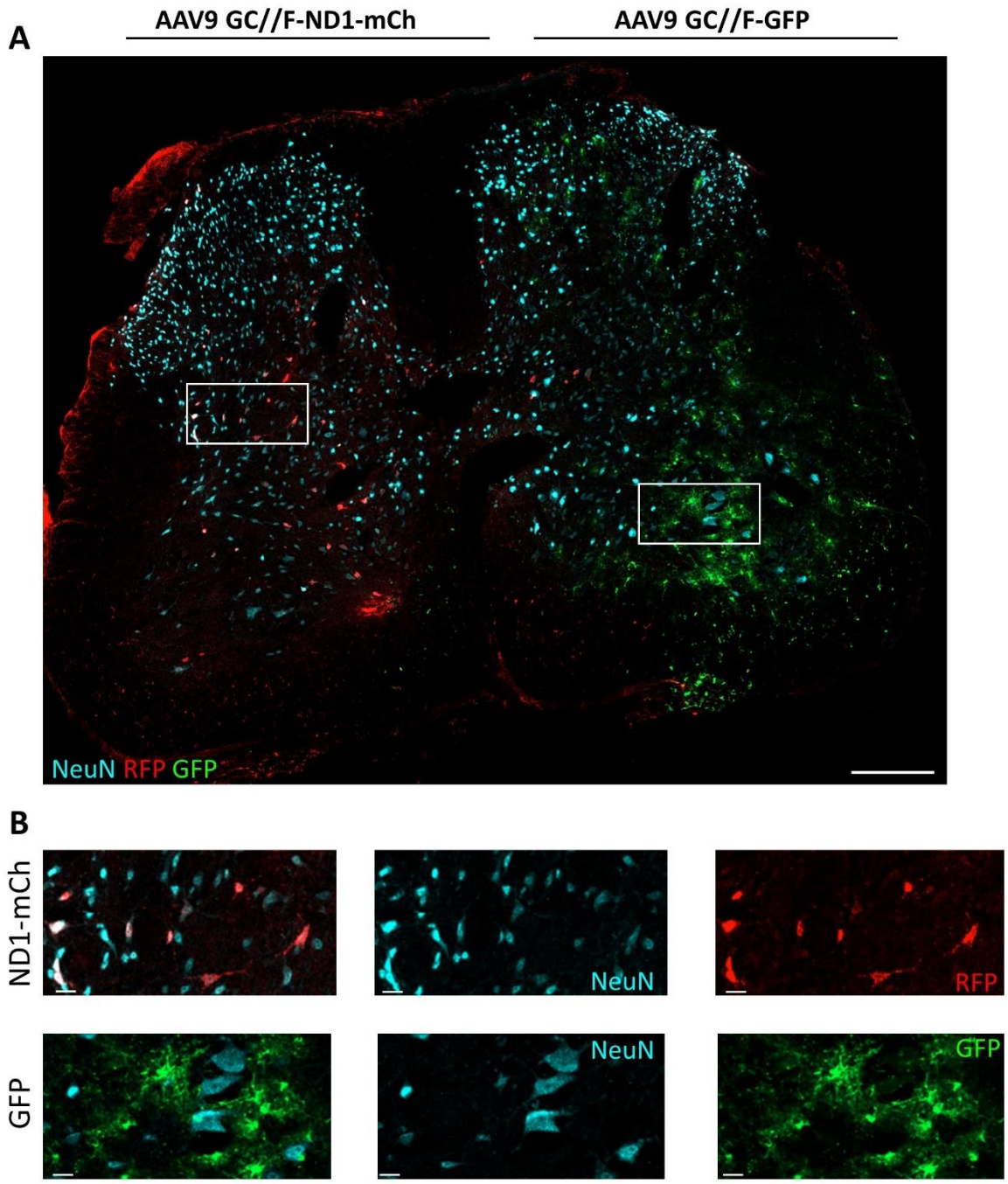

Figure 8. Cell Characterization in Two Sided ND1-mCh and GFP Spinal Cord Injection
(A) Coronal section of SOD1 G93A mouse two weeks after 2 sided injection. The left side is infected with the ND1-mCherry experimental virus while the right side is infected with the GFP control virus. Scale bar is 200 μm **(B)** cells expressing the mCherry reporter protein (red) used in the ND1 virus costain with the neuronal marker NeuN (blue), while cells expressing the GFP reporter protein (green) used in the control virus appear astrocytic in nature and do not co-stain with NeuN. Scale bar is 20 μm. Images provided by Yuan Liu

In a separate experiment, SOD1 G93A mice were sacrificed at earlier time points after injection to gain a better understanding of the cell transformation from astrocyte to neuron after infection with the ND1 virus. For this set of experiments, a new virus construct was used with ND1-GFP being directly driven by the EF1α promoter. The elongation Factor 1α (EF1α) gene is active in many tissues including the brain, placenta, lung, liver, kidney and pancreas [38]. In the brain, it is reported to be expressed both in neurons and astrocytes [39]. When injected into the spinal cord of SOD1 G93A mice, we found the virus to express in both neurons and astrocytes. At only 8 days after infection with this virus, transitional cells were able to be observed that had characteristics of both neurons and astrocytes (Figure 9). In a wildtype or control-injected mouse, GFAP and NeuN staining will never overlap as they are very specific to their respective cell types. Thus, it is significant to observe a transitional cell co-stained with NeuN, GFAP, and

GFP, suggesting that is has been infected by the ND1 virus and is in the process of converting from an astrocyte to neuron.

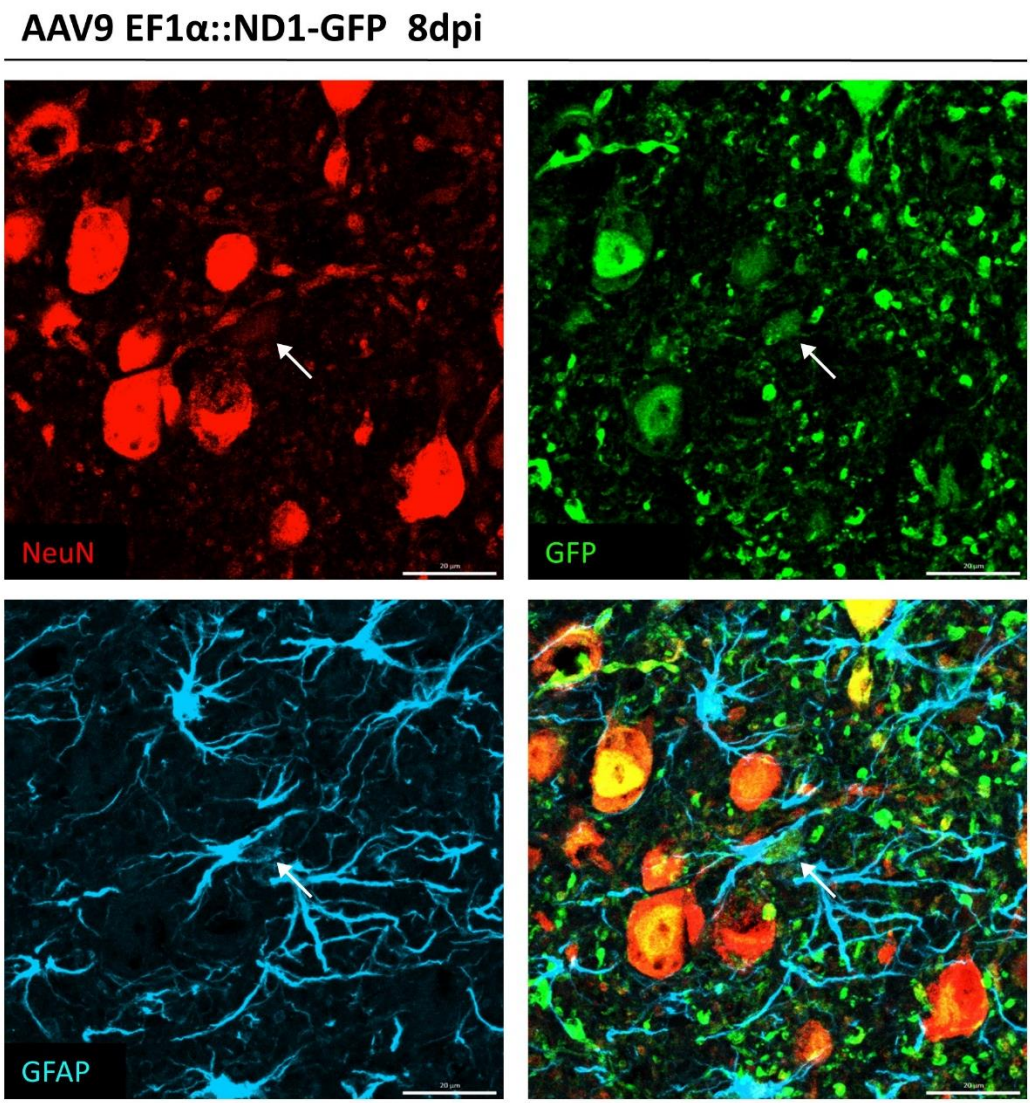

Figure 9. Transitional Cell in ND1 Injected Mouse
A transitional cell (white arrow) is observed at 8 dpi in a ND1 injected SOD1 G93A mouse. The cell expressed the ND1 virus reporter protein GFP (green) and co-localizes with neuronal marker NeuN (red) and glial marker GFAP (blue). Scale bar is 20 μm. Images provided by Yuan Liu

The EF1α directly driven ND1-GFP virus was also used to track the infection status over time and to observe the changes in the population of infected cells. For this experiment, a control

virus was also developed without the ND1 gene but with the GFP reporter so that the initial population of infected cells could be determined. At 3 dpi, both the control injection and the ND1 injection appeared to have similar expression patterns. Most cells presented with astrocytic morphology and co-stained with GFAP (Figure 10A, 10B). In addition, many GFP signals in both the control and experimental group co-stained with the oligodendrocyte precursor cell (OPC) marker Olig2. Besides astrocytes and OPCs, there was weak expression of GFP seen in neurons as well. However, we found the expression of the EF1α directly driven GFP and ND1-GFP to be strongest in astrocytes and OPCs at this time point.

At 8 dpi, the expression pattern in cells began to change. In the ND1 injected mice, nearly all of the infected cells present with neuronal morphology and co-stain with NeuN (Figure 10C). Very few cells are found to co-localize with GFAP at this point, indicating that there are little to no infected astrocytes at 8 dpi. Later, at 3 wpi, the expression pattern is similar. Nearly all of the infected cells were found to co-stain with NeuN while no GFP could be detected in astrocytes at this point (Figure 10D). Taken together, this time course data supports the theory that ND1 expression in astrocytes is able to convert many of them into neurons by 3 weeks post injection.

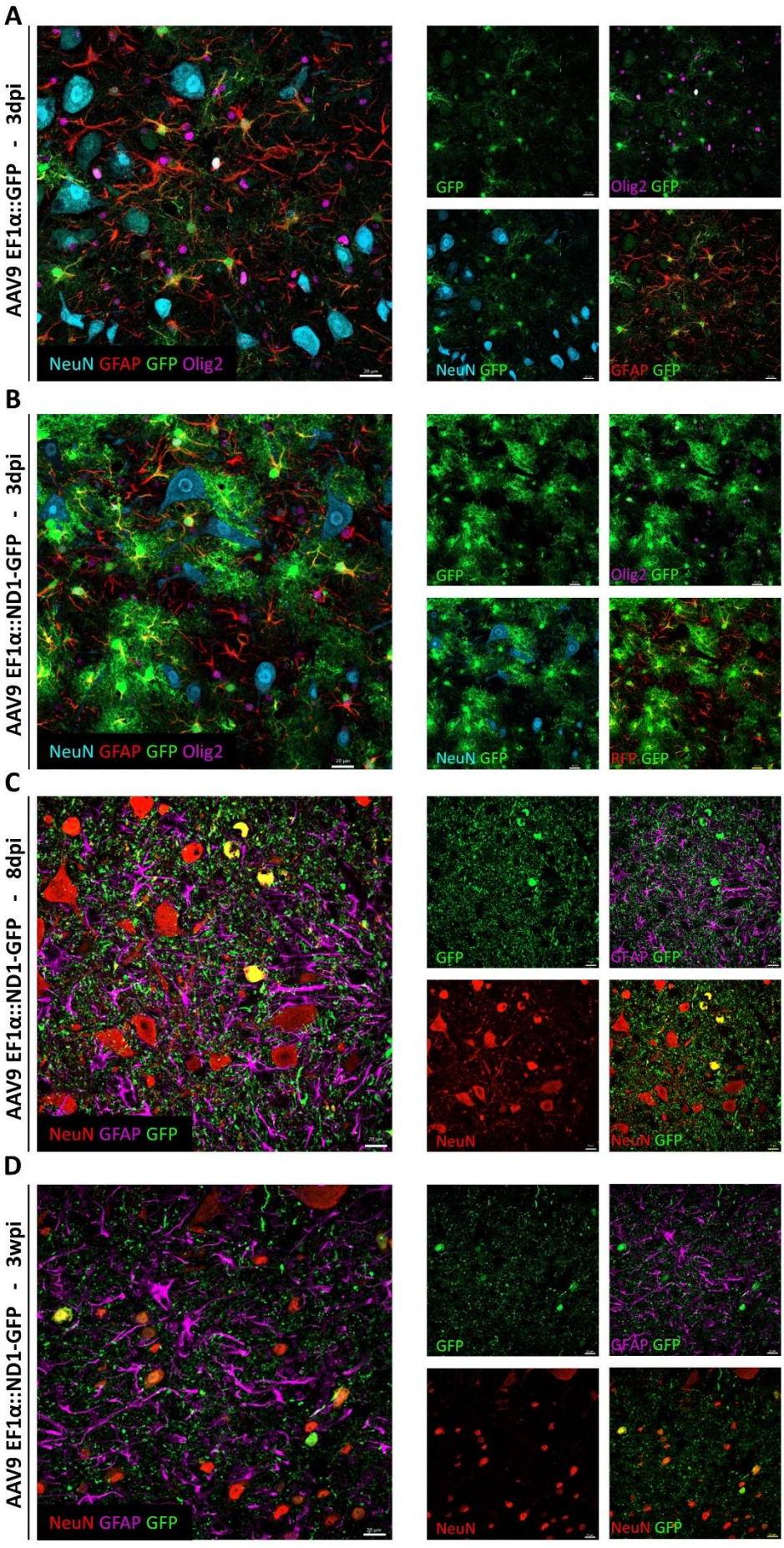
A
AAV9 EF1α::GFP - 3dpi
NeuN GFAP GFP Olig2
GFP
Olig2 GFP
NeuN GFP
GFAP GFP
B
AAV9 EF1α::ND1-GFP - 3dpi
NeuN GFAP GFP Olig2
GFP
Olig2 GFP
NeuN GFP
RFP GFP
C
AAV9 EF1α::ND1-GFP - 8dpi
NeuN GFAP GFP
GFP
GFAP GFP
NeuN
NeuN GFP
D
AAV9 EF1α::ND1-GFP - 3wpi
NeuN GFAP GFP
GFP
GFAP GFP
NeuN
NeuN GFP

Figure 10. Status of AAV9::EF1α Infection
(A) GFP control injection status at 3 dpi. Cells expressing the control virus reporter protein GFP (green) mostly appear astrocytic in nature and were found to co-localize with the glial marker GFAP (red) and OPC marker Olig2 (purple). Moreover, light GFP expression was observed to co-localize with the neuronal marker NeuN (blue), indicating a low level of expression of the reporter protein in neurons. **(B)** ND1-GFP injection status 3 dpi. The infection status appears similar to the 3dpi control injection. Most cells expressing the ND1 virus reporter protein GFP appear astrocytic in nature and are seen to co-localize with the glial marker GFAP (red) and OPC marker Olig2 (purple). Less GFP expressing cells are seen co-localizing with the neuronal marker NeuN (blue), indicating little to no ND1-GFP virus expression in neurons at 3 dpi. **(C)** ND1-GFP injection status 8 dpi. At this time point, the population of cells expressing the ND1 virus reporter protein GFP (green) has begun to change. GFP expressing cells are observed to co-localize with the neuronal marker NeuN (red), while no overlap between GFP expressing cells and the glial marker GFAP (purple) was observed. In addition, many small GFP+ fibers are observed throughout the entire image, possibly from the axonal and dendritic projections of GFP+ neurons. **(D)** ND1-GFP injections status 3 wpi. Cells expressing the ND1 virus reporter protein GFP (green) co-localize with the neuronal marker NeuN (red) but do not co-localize with the glial marker GFAP (purple). Additionally, many GFP+ fibers are still observed at this time point. Scale bar is 20 μm. Images provided by Yuan Liu

The EF1α::ND1-GFP experiments were also used to investigate the potential beneficial effects of ND1 in the ALS mouse model. Mice were injected at 8 weeks of age, therefore at 3 wpi they would be 11 weeks of age, which is old enough to begin showing symptoms of neuronal degeneration related to ALS. At this time point, differences in neuronal protein expression patterns can be found between the ND1-injected side and the non-injected side of the spinal cord, specifically in ChAT staining (Figure 11A). Healthy motor neurons are characterized by bright, diffuse ChAT staining in the cell body and many bright puncta stained with ChAT covering the cell body. At 3 wpi, we found the ChAT staining of the motor neurons to be brighter and healthier looking on the ND1-injected side compared to the non-injected side. Moreover, motor neurons on the ND1-injected side that were close to the injection point appeared with brighter ChAT staining, and the brightness decreased as a function of distance from the injection (Figure 11B). It is unlikely that all of these motor neurons are newly generated motor neurons, however the EF1α driven virus was able to infect neurons as well so this is

expected. The brighter, healthier looking ChAT staining on the ND1-injected side suggests ND1 may have a beneficial or protective effect on endogenous neurons.

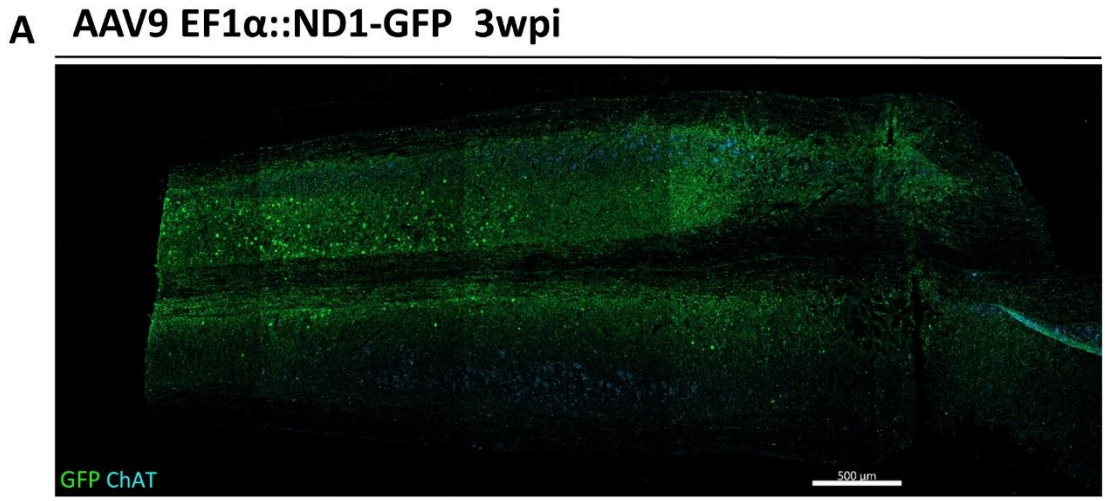

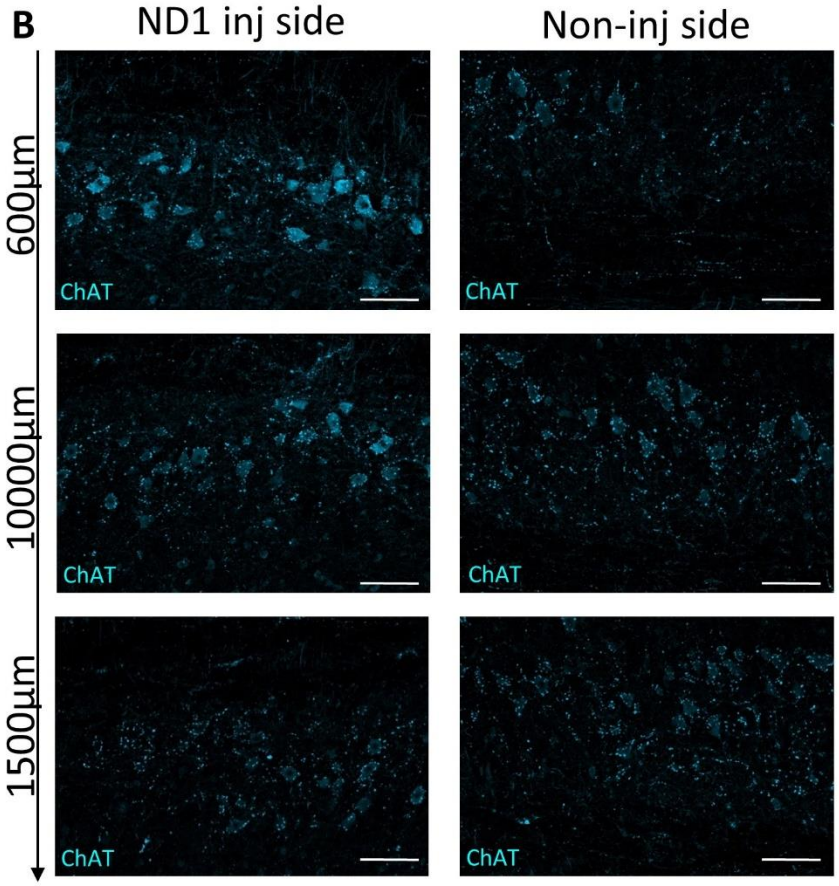

Figure 11. ChAT Staining Appears Brighter in ND1 Injected Spinal Tissue
(A) Overview of ND1-GFP infection at 3 wpi in a SOD1 G93A mouse. As pictured, the top side is the ND1-injected side as visualized by the greater expression of the GFP reporter protein (green). Scale bar is 500 μm. **(B)** Staining of the lateral motor columns in the injected and non-injected sides of the spinal cord for the motor neuron marker ChAT (blue). Distances represent lateral distance from point of injection. As the distance from the point of injection increases on the injected side, ChAT staining becomes weaker and resembles that of the non-injected side, which stays uniformly weak. Scale bar is 100 μm. Images provided by Yuan Liu

Chapter 4

Discussion

Astrocyte-to-Neuron Conversion

It was the goal of this paper to demonstrate the ability of the NIL and ND1 viruses to convert astrocytes into neurons *in vivo* in spinal cord injury and ALS mouse models. The best evidence for direct conversion is seen in the changing population of infected cells over time and the presence of transitional cells. As we observed, many of the cells infected with our AAV9 GFAP::cre system were GFAP+ astrocytes, just as the system was designed. However, by 4 weeks, no GFAP+ infected cells could be found. Instead, all of the infection was found in NeuN+ neurons. Therefore, all of the infected astrocytes found in the early time point either stopped expressing the reporter protein, died, or transformed into neurons. While the AAV9 EF1α system was able to infect Olig2+ OPCs and some NeuN+ neurons, the lack of GFAP+ astrocytes found at later time points leaves the same three possibilities of loss of reporter protein, death, or transformation as presented with the GFAP::cre system.

The observation of transitional cells is the key piece of evidence that suggests the infected astrocytes are in fact converting rather than dying or losing expression of the reporter protein. As ND1 activates many neuronal genes and begins to downregulate several astrocytic genes, it would make sense there would be a point where a transitioning cell would express protein markers for both neurons and astrocytes. Moreover, we have never been able to observe the overlap of GFAP and NeuN in any cells in a wild type or control-injected sample. All of this suggests that these GFAP+/NeuN+ cells are unique to our experimental conditions and likely represent an intermediate state in the process of neuronal conversion.

Despite all of this evidence, it can still not be unequivocally concluded that the NIL and ND1 viruses were able to convert astrocytes into neurons *in vivo*. One alternative explanation of the changing infected cell population is leakage of the virus into endogenous neurons. In both virus models, it was observed that the virus was able to infect and express its protein products in neurons. With the EF1α system, this was less of a concern because EF1α was expected to have some sort of expression in neurons. However, with our GFAP::cre system, we were able to find neurons expressing mCherry even when they were injected with the control virus which should be unable to express cre in neurons or convert astrocytes. As discussed earlier, this leakage can be seen taking place in the areas outside of the heavily damaged area in the SCI samples (Figure 3). If the virus was somehow able to express the cre recombinase plasmid in endogenous neurons, then these neurons would be able to properly orient and successfully express the ND1/NIL genes. Thus there is the potential that some neurons expressing the reporter proteins in the experimental groups were endogenous rather than newly generated.

To combat this problem of leakage and provide more concrete evidence of astrocyte-to-neuron conversion in the spinal cord, a better knowledge of the factors impacting leakage is needed. One possibility is that GFAP is not as selective for glia as previously thought. Knockout experiments have shown that loss of GFAP has an impact on neuronal morphology and studies of Alzheimer's disease suggest neurons can express GFAP in a degenerative disease model [40,41]. By some mechanism, it appears GFAP is related to neurons, even though it may be very slightly. It is possible that damaged neurons in our SCI and ALS mouse models are able to express modest levels of GFAP, thus allowing them to produce cre recombinase and express ND1/NIL when infected. If a more specific promoter to astrocytes were used to express cre, then perhaps

the leakage problem could be solved and all neurons showing the reporter protein could be taken as newly generated neurons from astrocytic origins.

Beneficial Effect of ND1

While the problem of leakage needs to be solved before direct conversion *in vivo* can be conclusively determined, the beneficial effect of our conversion technologies in SCI and ALS mouse models can be examined with the available data. For example, in our SCI model, a significantly greater number of neurons were found in the severely damaged area at 4wps in the NIL injected sample compared to the control injected sample. Whether these are newly converted neurons or leaked endogenous neurons, the fact remains there is less neuron loss in the NIL treated sample four weeks after the stab injury. NGN2 has been reported to have a neuroprotective effect in other CNS injury models, such as ischemia reperfusion-injury [42]. Perhaps the expression of NGN2 in converted and even leaked neurons in our model was able to provide some protection against the toxic injury core, which would lead to a greater number of surviving neurons in the treatment group.

A potential beneficial effect was also observed in our ND1 injected ALS mice with brighter, healthier looking ChAT signals on the injected side of the spinal cord when compared to the non-injected side. Again, a protective effect may be at play as studies report that the expression of ND1 can have neuroprotective properties, for example in a Parkinson's disease model [43]. The EF1α delivery method of ND1 in ALS mouse has the ability to infect endogenous neurons, therefore it is possible ND1 provided protection to many endogenous motor neurons,

resulting in healthier looking ChAT signal at 11 weeks of age compared to the non-injected side of the spinal cord.

Limitations and Considerations

While decreased neuron loss in our SCI model and healthier ChAT signals in our ALS model are positive signs that point towards a beneficial impact from our treatments, there needs to be a much greater amount of research to further understand and support these claims. Firstly, these are very limited measures of a beneficial impact. A true beneficial impact would see improvement of many other markers in the injury and disease models. For example, reduction of astrogliosis in the SCI model would be a desirable impact of treatment; however, we have yet to observe that as a result of NIL or ND1 injections. In our ALS model, negative changes like microgliosis, reduced vGlut1 density, and sciatic nerve degeneration represent targets for treatment. Currently, we have been unable to observe improvement in these pathological signs of disease progression after ND1 injection. More work needs to be done in examining these other markers of the disease to truly determine if ND1 and NIL treatment is providing any kind of beneficial impact beyond the generation of new neurons.

Of course, the ultimate goal of treatment with ND1 and NIL is for the mice to return to a normal phenotypic behavior after injury or onset of disease. If the generation of new neurons does not actually result in behavioral improvement, then the treatment will not be very successful. We have specifically studied the phenotype of ALS mice using RotaRod and hangwire experiments. As of right now, though, our behavioral tests have remained inconclusive about the impact of ND1 in an ALS mouse model. Our current data simply has too much

variation in it to determine a significant result, whether it is beneficial or not. At the time of writing, we are currently conducting more behavioral tests with revised methods on a large group of ND1 treated SOD1 G93A mice, and we hope to collect enough data to definitively answer the question of behavioral improvement.

Another issue limiting our ability to see significant, wide ranging beneficial impacts in the ALS mouse model is the nature of our focal injection of ND1. As a neurodegenerative disease, ALS cannot be confined to a specific area of the spinal cord. In actuality, the damage caused by the disease is diffuse and spread throughout the spinal cord. Thus, a focal injection may not be enough to positively impact the entire spinal cord. In an effort to address this problem, we have since begun using intrathecal injections to administer ND1. Preliminary data from our experiments suggests this method of administering virus is able to achieve global infection of the spinal cord, however its efficacy in converting astrocytes and providing a beneficial impact are still being examined.

Finally, the leakage of virus into preexisting neurons when using the GFAP::cre system is limiting our ability to confidently conclude which infected neurons are newly generated and which are leaked. In previous experiments, members of the lab used a retrovirus to deliver ND1. As retrovirus can only infect dividing cells, neurons would never be infected and leakage was not a problem. However, we found the infection rate to be very low in our retrovirus experiments, thus prompting the change to the AAV9 virus, which has been shown to have high infection rates in both astrocytes and neurons in the CNS[44,45]. We found this to be true in our experiments as well; however, if AAV9 is going to continue to be used, new methods must be developed to decisively determine whether a neuron is newly generated or leaked.

Overall, many of these limitations can be overcome by increasing the sample size and data set. While a promising start, the data in this paper represent patterns and trends that have been observed; however, many more replicates will be needed to conclusively determine if there is a true beneficial effect of ND1 and NIL treatment, and if so to what extent.

Concluding Remarks

The data discussed in this paper suggest NIL and ND1 have potential to be legitimate treatments for SCI and ALS. Survival of more neurons after stab injury, the presence of transitioning cells, and motor neurons with healthier cholinergic profiles have all been observed from these treatments , but more data must be collected to confirm and expand upon these findings. Ultimately, the *in vivo* conversion of astrocytes to neurons is a powerful technology with great promise in the treatment of neurodegenerative disease and injuries. Compared to the current treatments for SCI and ALS which can only reduce injury toxicity or prolong disease progression, our technology has the potential to actually form new connections and replace lost neurons in the hope of a full recovery.

BIBLIOGRAPHY

1. Lee, B. B., Cripps, R. A., Fitzharris, M. & Wing, P. C. The global map for traumatic spinal cord injury epidemiology: update 2011, global incidence rate. *Spinal Cord* **52,** 110–116 (2014).
2. *Spinal Cord Injury Facts and Figures at a Glance*. (2018).
3. Sekhon, L. H. S. & Fehlings, M. G. Epidemiology, Demographics, and Pathophysiology of Acute Spinal Cord Injury. *Spine (Phila. Pa. 1976).* **26,** S2–S12 (2001).
4. Rolls, A., Shechter, R. & Schwartz, M. NEURON - GLIA INTERACTIONS - OPINION The bright side of the glial scar in CNS repair. *Nat. Rev. Neurosci.* **10,** 235-U91 (2009).
5. Silva, N. A., Sousa, N., Reis, R. L., Nio, A. & Salgado, J. From basics to clinical: A comprehensive review on spinal cord injury. (2014). doi:10.1016/j.pneurobio.2013.11.002
6. Chiò, A. *et al.* Prognostic factors in ALS: A critical review. *Amyotroph. Lateral Scler.* **10,** 310–23 (2009).
7. Al-Chalabi, A. & Hardiman, O. The epidemiology of ALS: A conspiracy of genes, environment and time. *Nat. Rev. Neurol.* **9,** 617–628 (2013).
8. Andersen, P. M. & Al-Chalabi, A. Clinical genetics of amyotrophic lateral sclerosis: What do we really know? *Nat. Rev. Neurol.* **7,** 603–615 (2011).
9. Taylor, J. P., Brown, R. H. & Cleveland, D. W. Decoding ALS: From genes to mechanism. *Nature* **539,** 197–206 (2016).
10. Miller, R., Mitchell, J., Lyon, M. & Moore, D. Riluzole for amyotrophic lateral sclerosis (ALS)/motor neuron disease (MND). *Amyotroph. Lateral Scler. Other Mot. Neuron*

Disord. **4,** 191–206 (2003).

11. Rothstein, J. D. Edaravone: A new drug approved for ALS. *Cell* **171,** 725 (2017).
12. Abe, K. *et al.* Confirmatory double-blind, parallel-group, placebo-controlled study of efficacy and safety of edaravone (MCI-186) in amyotrophic lateral sclerosis patients. *Amyotroph. Lateral Scler. Front. Degener.* **15,** 610–617 (2014).
13. Takahashi, K. & Yamanaka, S. Induction of Pluripotent Stem Cells from Mouse Embryonic and Adult Fibroblast Cultures by Defined Factors. *Cell* **126,** 663–676 (2006).
14. Takahashi, K. *et al.* Induction of Pluripotent Stem Cells from Adult Human Fibroblasts by Defined Factors. *Cell* **131,** 861–872 (2007).
15. Hallett, P. J. *et al.* Successful Function of Autologous iPSC-Derived Dopamine Neurons following Transplantation in a Non-Human Primate Model of Parkinson's Disease. *Cell Stem Cell* **16,** 269–274 (2015).
16. Tatarishvili, J. *et al.* Human induced pluripotent stem cells improve recovery in stroke-injured aged rats. *Restor. Neurol. Neurosci.* **32,** 547–58 (2014).
17. Jin, X., Lin, T. & Xu, Y. Stem Cell Therapy and Immunological Rejection in Animal Models. *Curr. Mol. Pharmacol.* **9,** 284–288 (2016).
18. Okano, H. *et al.* Steps Toward Safe Cell Therapy Using Induced Pluripotent Stem Cells. *Circ. Res.* **112,** 523–533 (2013).
19. Knoepfler, P. S. Deconstructing Stem Cell Tumorigenicity: A Roadmap to Safe Regenerative Medicine. *Stem Cells* **27,** 1050–1056 (2009).
20. Guo, Z. *et al.* Cell Stem Cell Article In Vivo Direct Reprogramming of Reactive Glial Cells into Functional Neurons after Brain Injury and in an Alzheimer's Disease Model. (2014). doi:10.1016/j.stem.2013.12.001

21. Su, Z., Niu, W., Liu, M.-L., Zou, Y. & Zhang, C.-L. In vivo conversion of astrocytes to neurons in the injured adult spinal cord. *Nat. Commun.* **5,** 3338 (2014).

22. Li, X. *et al.* Small-Molecule-Driven Direct Reprogramming of Mouse Fibroblasts into Functional Neurons. *Cell Stem Cell* **17,** 195–203 (2015).

23. Brulet, R. *et al.* NEUROD1 Instructs Neuronal Conversion in Non-Reactive Astrocytes. *Stem Cell Reports* **8,** 1506–1515 (2017).

24. Liu, M.-L. *et al.* Small molecules enable neurogenin 2 to efficiently convert human fibroblasts into cholinergic neurons. *Nat. Commun.* **4,** 2183 (2013).

25. Lee, J. E. *et al.* Conversion of Xenopus ectoderm into neurons by NeuroD, a basic helix-loop-helix protein. *Science* **268,** 836–44 (1995).

26. Gao, Z. *et al.* Neurod1 is essential for the survival and maturation of adult-born neurons. *Nat. Neurosci.* **12,** 1090–1092 (2009).

27. Pleasure, S. J., Collins, A. E. & Lowenstein, D. H. Unique expression patterns of cell fate molecules delineate sequential stages of dentate gyrus development. *J. Neurosci.* **20,** 6095–105 (2000).

28. Lee, S.-K., Lee, B., Ruiz, E. C. & Pfaff, S. L. Olig2 and Ngn2 function in opposition to modulate gene expression in motor neuron progenitor cells. *Genes Dev.* **19,** 282–94 (2005).

29. Helms, A. W. *et al.* Sequential roles for Mash1 and Ngn2 in the generation of dorsal spinal cord interneurons. *Development* **132,** 2709–19 (2005).

30. Tu, P. H. *et al.* Transgenic mice carrying a human mutant superoxide dismutase transgene develop neuronal cytoskeletal pathology resembling human amyotrophic lateral sclerosis lesions. *Proc. Natl. Acad. Sci. U. S. A.* **93,** 3155–60 (1996).

31. Gurney, M. E. *et al.* Motor neuron degeneration in mice that express a human Cu,Zn superoxide dismutase mutation. *Science* **264,** 1772–5 (1994).

32. Mazzoni, E. O. *et al.* Synergistic binding of transcription factors to cell-specific enhancers programs motor neuron identity. *Nat. Neurosci.* **16,** 1219–1227 (2013).

33. Bruijn, L. I. *et al.* ALS-linked SOD1 mutant G85R mediates damage to astrocytes and promotes rapidly progressive disease with SOD1-containing inclusions. *Neuron* **18,** 327–38 (1997).

34. Alexianu, M. E., Kozovska, M. & Appel, S. H. Immune reactivity in a mouse model of familial ALS correlates with disease progression. *Neurology* **57,** 1282–9 (2001).

35. Watanabe, M. *et al.* Histological Evidence of Protein Aggregation in Mutant SOD1 Transgenic Mice and in Amyotrophic Lateral Sclerosis Neural Tissues. *Neurobiol. Dis.* **8,** 933–941 (2001).

36. Schütz, B. Imbalanced excitatory to inhibitory synaptic input precedes motor neuron degeneration in an animal model of amyotrophic lateral sclerosis. *Neurobiol. Dis.* **20,** 131–140 (2005).

37. Tian, F. *et al.* Monitoring peripheral nerve degeneration in ALS by label-free stimulated Raman scattering imaging. *Nat. Commun.* **7,** 13283 (2016).

38. Fagerberg, L. *et al.* Analysis of the Human Tissue-specific Expression by Genome-wide Integration of Transcriptomics and Antibody-based Proteomics. *Mol. Cell. Proteomics* **13,** 397–406 (2014).

39. Yaguchi, M. *et al.* Characterization of the Properties of Seven Promoters in the Motor Cortex of Rats and Monkeys After Lentiviral Vector-Mediated Gene Transfer. *Hum. Gene Ther. Methods* 333–344 (2013). doi:10.1089/hgtb.2012.238

40. McCall, M. A. *et al.* Targeted deletion in astrocyte intermediate filament (Gfap) alters neuronal physiology. *Proc. Natl. Acad. Sci. U. S. A.* **93,** 6361–6 (1996).

41. Hol, E. M. *et al.* Neuronal expression of GFAP in patients with Alzheimer pathology and identification of novel GFAP splice forms. *Mol. Psychiatry* **8,** 786–796 (2003).

42. Deng, B. *et al.* Targeted delivery of Neurogenin-2 protein in the treatment for cerebral ischemia-reperfusion injury. *Biomaterials* **34,** 8786–8797 (2013).

43. Singh, S., Mishra, A. & Shukla, S. ALCAR Exerts Neuroprotective and Pro-Neurogenic Effects by Inhibition of Glial Activation and Oxidative Stress via Activation of the Wnt/β-Catenin Signaling in Parkinsonian Rats. *Mol. Neurobiol.* **53,** 4286–4301 (2016).

44. Lykken, E. A., Shyng, C., Edwards, R. J., Rozenberg, A. & Gray, S. J. Recent progress and considerations for AAV gene therapies targeting the central nervous system. *J. Neurodev. Disord.* **10,** 16 (2018).

45. Foust, K. D. *et al.* Intravascular AAV9 preferentially targets neonatal neurons and adult astrocytes. *Nat. Biotechnol.* **27,** 59–65 (2009).

ACADEMIC VITA

Education

Schreyer Honors College
The Pennsylvania State University **University Park, PA**
Eberly College of Science
Class of 2019
Biology Major, Neuroscience Option
Deafness and Hearing Studies Minor
Awards: Headings Scholarship, Evan Pugh Scholar Award, Dean's List Fall 2015 - present

Activities and Work Experience

Chen Lab **University Park, PA**
Research Assistant *February 2016 - Present*

- Investigated the direct, in-vivo conversion of glial cells into functional neurons in the spinal cord after stab injury and presented results in front of lab leaders and peers during biweekly lab meetings
- Explored the use of conversion technology to develop a beneficial environment within the spinal cord to either regenerate or support the survival of motor neurons in an ALS mouse model
- Assisted in laminectomy surgery and stereotaxic injections of mice requiring expertise in administration of injections, suturing of wounds, and adherence to sterile technique
- Mastered various histological procedures including immunostaining and confocal imaging

Department of Biology **University Park, PA**
Assistant Teaching Assistant *August 2016 – May 2017*

- Demonstrated extensive knowledge of core biology components for Biology 110 and 240 and relevant laboratory procedures through direct communication with students in a classroom setting
- Collaborated with faculty and graduate Teaching Assistants to coordinate labs for more than 90 students

Team and Volunteer Experience

Penn State Dance Marathon **University Park, PA**
Hospitality and Finance Committee Member *October 2016 – March 2019*

- Worked within a team of 25 members to prepare and serve meals to dancers and families during THON weekend
- Gained experience in customer relations through volunteering at concession stands within the Bryce Jordan Center
- Developed and cultivated an active relationship with a Four Diamonds child and family through continuation of written correspondence, organizing gifts, and coordinating visits while serving as Penn Pal Chair

Double H Ranch **Lake Luzerne, NY**
Volunteer Counselor *July 2017 – August 2017*

- Double H Ranch is a summer camp which specializes in providing specialized programming to children facing life threatening illnesses
- Volunteered as Cabin Counselor for two weeks which included full time supervision of the children, daily preparation and serving of meals, and participation in adaptive techniques to make camp accessible for all children

- Responsible for children's medical needs including administering medication, providing personal care, and monitoring situations to avoid any allergens

Manna on Main Street **Lansdale, PA**
Volunteer *June 2017 – Present*

- Manna on Main Street is a food pantry, soup kitchen, and counseling center serving the Lansdale community
- Prepared and served meals, placed and cleaned tables, and scanned and bagged groceries for more than a hundred people per day

Relevant Coursework

- Neurobiology, Evolutionary Biology, Molecular Biology, Genetics, Organic Chemistry